Regional Environmental Change (2022) 22: 58
https://doi.org/10.1007/s10113-022-01920-4

ORIGINAL ARTICLE

Climate change impacts on future driving and walking conditions in Finland, Norway and Sweden

Nadine-Cyra Freistetter[1] · Erika Médus[1] · Marjo Hippi[2] · Markku Kangas[2] · Andreas Dobler[3] · Danijel Belušić[4,5] · Jukka Käyhkö[6] · Antti-Ilari Partanen[1]

Received: 18 December 2021 / Accepted: 20 March 2022 / Published online: 7 April 2022

Abstract

Road weather is a major concern for the public safety and health, industries and transport sectors. Half of the yearly 27,000 road and 50,000 pedestrian injuries in Finland, Norway and Sweden can be traced back to slippery road and walkway conditions. We simulated the climate change impacts on future roads and walkways for mid- and end-century in Finland, Norway and Sweden with the road weather model RoadSurf, driven by the regional climate model HCLIM38 with boundary data from two global climate models following the RCP8.5 scenario.

Our simulations for mid-century suggest strong road surface temperature increases, especially in southern Finland (+5.1 °C) and Sweden (+7.1 °C). Snowy and icy road surface conditions decreased by 23 percentage points, causing 18.5 percentage points less difficult driving conditions during the cold season. Zero-degree-crossing days mostly decreased in autumn and spring by up to 7 days and increased in winter by up to 5 days. Sidewalks mostly showed a decrease in slipperiness, but a five percentage point increase of water above ice layers on the sidewalks in winter, suggesting the slip-season might become shorter, but more slippery.

Our results are upper extreme estimates but can serve as a reference to help local decision-makers plan mitigation and adaptation measures ahead of time.

Keywords Road weather · Climate change impacts · Road safety · Pedestrian safety · Winter road maintenance · Climate modelling

Communicated by Georgios Zittis

✉ Nadine-Cyra Freistetter
nadine.freistetter@fmi.fi

Erika Médus
erika.medus@fmi.fi

Marjo Hippi
marjo.hippi@fmi.fi

Markku Kangas
markku.kangas@fmi.fi

Andreas Dobler
andreasd@met.no

Danijel Belušić
danijel.belusic@smhi.se

Jukka Käyhkö
jukka.kayhko@utu.fi

Antti-Ilari Partanen
antti-ilari.partanen@fmi.fi

[1] Finnish Meteorological Institute, Climate System Research, Erik Palménin aukio 1, 00560 Helsinki, Finland

[2] Finnish Meteorological Institute, Meteorological Research, Helsinki, Finland

[3] Norwegian Meteorological Institute, Bergen, Norway

[4] Swedish Meteorological and Hydrological Institute, Norrköping, Sweden

[5] University of Zagreb, Zagreb, Croatia

[6] Department of Geography and Geology, University of Turku, Turku, Finland

Introduction

Weather plays a crucial role for the transportation of passengers and goods (Norrman et al., 2000). Traffic accidents involving personal injury or death due to slippery conditions account for up to 50% of the over 27,000 injuries in recent years in Finland, Norway and Sweden (FNS). Medical costs and economic production losses arising from these accidents sum up to €16.2 billion yearly (European Commission Directorate-General for Mobility and Transport & CE Delft, 2019; International Traffic Safety Data and Analysis Group, 2020a, b, c, d; Statistics Finland, 2021; Statistics Sweden, 2019). An often-overlooked burden is posed by pedestrian slip injuries. A majority of the 50,000 slips that need medical attention yearly are caused by slippery conditions (Elvik et al., 2009; Elvik & Bjørnskau, 2019; Hippi et al., 2020; Port and Ocean Engineering under Arctic Conditions (POAC) (2009).

These accidents cannot be prevented even with full winter-time road maintenance (Norrman et al., 2000). Therefore, reducing accident numbers by informing the public about hazardous road weather is important for the public health sector. Road maintenance and transport sectors benefit from road weather forecasts as well, for planning ahead their actions and reducing costs (Juga et al., 2013; Keskinen, 1980; Nurmi et al., 2013).

Currently, public authorities are working with real-time road weather observations and short-term weather forecasts to issue warnings when the road weather is expected to worsen. Road weather models typically predict the road surface temperature and the amount of snow, ice or water on the surface, and in some cases also friction and driving condition (Juga et al., 2013; Kangas et al., 2015). Regional road weather models have been developed in several countries to improve the regional accuracy (Chapman et al., 2001; Crevier & Delage, 2001; Fujimoto et al., 2012; Jacobs & Raatz, 2007; Kangas et al., 2015; Yang et al., 2012).

As climate change has been posing far-reaching challenges on the transport sector worldwide (Forzieri et al., 2018; Hori et al., 2018; Matthews et al., 2017), road planners and maintenance operators are assessing the monetary funds needed to manage (either current or soon-arising) regional climate change impacts on the transport sector. Such challenges include shifts in more frequent extreme weather, safe transport routes, time and locality of accidents, shifts in tourism and agriculture and pavement material damage and road maintenance changes. (Andersson & Chapman, 2011a; Axelsen et al., 2016; Balston et al., 2017; Koetse & Rietveld, 2009). Particularly in high northern latitudes like Northern Europe or Canada, where winter road maintenance is both a necessity and a big cost point, climate change is estimated to have stronger impacts due to arctic amplification (Screen, 2014).

Whilst weather models produce road weather forecasts for the near future and help manage immediate risks, they are not capable of portraying long-term developments beyond a few weeks. Climate models on the other hand give estimates for many decades or even centuries ahead and can simulate different climate change scenarios. Driving road weather models with climate models therefore can help road management and authorities to better plan ahead for the arising challenges and opportunities of road management in the far future (Matthews et al., 2017; McSweeney et al., 2016). Our predecessor study by Toivonen et al. (2019) confirmed that the Finnish road weather model RoadSurf (Finnish Meteorological Institute, Kangas et al., 2015) produced accurate historical road temperature estimates for Finland when driven with the cycle 38 of the regional climate model HARMONIE-Climate (HCLIM38) and thereby set the grounds for this study.

We expand upon Toivonen et al. (2019) by exploring future road weather under a climate change scenario and adding the Norwegian and Swedish domains. We assess (1) whether forcing with the computationally more expensive high-resolution regional climate model HCLIM38-AROME configuration (3 km grid resolution) provides considerable benefits over the HCLIM38-ALADIN configuration (12 km grid) and, thereafter, we explore (2) the climate change impacts on roads in FNS by assessing possible future regional and temporal developments of average road surface temperatures, road surface conditions and driving and walking conditions, as well as zero-degree-crossings under climate change in reference to the historical period (1986–2005).

Data sources and models

Our main model was the road weather model RoadSurf (Kangas et al., 2015) driven by regional climate model simulations from the cycle 38 of HARMONIE-Climate (HCLIM38; Belušić et al., 2020). Since RoadSurf cannot produce its own climate scenario, it needs external data to provide the meteorological boundary data. To provide these data, we used three different sources: one reanalysis dataset and two CMIP5 global climate models, EC-Earth (ECE) and GFDL that considerably differed in their climate change predictions for the Nordics. See below for details about the models and data.

RoadSurf model and data

RoadSurf is an energy balance model that predicts driving conditions for the next 24 h. It estimates (1) the road surface

temperature, (2) friction and (3) storages on the road (water, snow, ice, frost in water mm-equivalent), and from these (4) road surface condition and (5) driving conditions (driving difficulty derived from a combination of weather and road surface conditions) (Kangas et al., 2015).

The model calculates the vertical heat fluxes between the atmosphere and the road surface by means of turbulence (including traffic-induced), generalised soil material properties and meteorological input parameters. The meteorological input parameters, taken from HCLIM38 regional model output, include 2-m air temperature, precipitation, relative humidity, wind speed and downwelling shortwave and longwave radiation with a time resolution of 1 h. Hydrological processes, including freezing, melting, evaporation, sublimation, run-off from the surface and accumulation of rain and snow, are parameterized. RoadSurf assumes a flat horizontal paved surface over the whole domain with similar deep-ground properties, without elements shading the road, such as trees. Topography, water bodies or forests are implicitly accounted for through the HCLIM38 input data.

Traffic is simulated as a spatially constant atmospheric turbulence on the ground with a larger value for daytime and a smaller one for night. Traffic reduces and changes the storages, e.g. by compressing snow into ice, whilst unpacked snow is assumed to be partly blown away by the wind. The model assumes neither salting nor road maintenance and, therefore, overestimates snow and ice storages on the road (Toivonen et al., 2019). This is justified as RoadSurf is commonly used to warn about the possibility of hazardous driving conditions, as a call to action for the regional road management (Kangas et al., 2015). Despite these overestimations, however, Toivonen et al. (2019) showed that RoadSurf reproduced observed road weather conditions in Finland (2002–2014) well when driven by HCLIM38. Furthermore, RoadSurf has been further developed to predict pedestrian sidewalk conditions (walking difficulty) (Hippi et al., 2020).

This study expands upon Toivonen et al. (2019) by exploring a future scenario of driving as well as pedestrian conditions and additional countries. Our study employed version 6.60b of RoadSurf with a few minor adjustments made in this study. We focused on four output variables: (1) road surface temperature (T_{RS}) (from which zero-degree-crossing days were derived); (2) road surface condition: dry, damp, wet, snow, frost, icy and partly icy; (3) driving condition: normal, difficult and very difficult; (4) pedestrian condition: normal, slippery (slipperiness may occur), very slippery due to foot-packed snow (VS I), very slippery due to water above ice layer (VS II) and very slippery due to snow above ice layer (VS III).

HARMONIE-Climate data

We used the HARMONIE-Climate "cycle 38" model runs (HCLIM38) (Belušić et al., 2020; Lind et al., 2016; Lindstedt et al., 2015) recently performed by the NorCP project for Northern Europe (Lind et al., 2020; Médus et al., 2022) with the packages (1) HCLIM38-AROME (3 km grid resolution) (Bengtsson et al., 2017; Seity et al., 2011; Termonia et al., 2018) and (2) HCLIM38-ALADIN (12 km grid resolution) (Termonia et al., 2018). A detailed description of the model can be found in Belušić et al. (2020).

The boundary data for HCLIM38-ALADIN were taken from either the global ERA-Interim reanalysis dataset (ERAI, 80 km grid resolution) (Dee et al., 2011) or from two CMIP5 global climate models (GCMs) from the Coupled Model Intercomparison Project–Phase 5 (CMIP5) (Taylor et al., 2012): EC-Earth (Hazeleger et al., 2010, 2011) and GFDL-CM3 (Donner et al., 2011; Griffies et al., 2011) (Table 1). We chose ECE and GFDL as driving GCMs as they cover the full range of temperature and precipitation projections for northern Europe in the RCP8.5 scenario in CMIP5 (Lind et al., 2022, in preparation).

Table 1 RoadSurf simulations presented in this paper. Combinations of one global ERA-Interim reanalysis (ERAI), two different global climate models (ECE, GFDL), two different HCLIM38-Configurations (AROME, ALADIN), two road-user modes (car, pedestrian) and four different time frames (historic 1986–2005, present 1998–2018, mid-century 2041–2060, end-century 2081–2100) were used

Boundary data	HCLIM38 configuration	Traffic mode	Time frame	Scenario	Purpose
ERAI	AROME	Car	1998–2018	Reanalysis	Evaluation
ECE	AROME	Car	1986–2005	Historical	Reference period
ERAI	ALADIN	Car and pedestrian	1998–2018	Reanalysis	Evaluation
ECE	ALADIN	Car and pedestrian	1986–2005	Historical	Reference period
ECE	ALADIN	Car and pedestrian	2081–2100	RCP 8.5	Future projection
GFDL	ALADIN	Car and pedestrian	1986–2005	Historical	Reference period
GFDL	ALADIN	Car and pedestrian	2041–2060 2081–2100	RCP 8.5	Future projection

The reanalysis-driven simulation was used for model evaluation purposes, whilst the GCM–driven runs were used to estimate the impacts of climate change.

Representative concentration pathway 8.5

The two global climate model simulations for HCLIM38 boundary data followed the representative concentration pathway (RCP) 8.5, which assumes continuing rising global greenhouse gas emissions, resulting in an expected increase of radiative forcing of 8.5 Wm^{-2} by 2100. This climate change scenario entails an estimated global temperature increase of + 1.8 °C (ECE)/ + 2.6 °C (GFDL) by mid-century (2046–2065) and up to + 3.5 °C/ + 4.7 °C by the end of the century (2081–2100), relative to temperatures in the historical period (1986–2005) (Stocker et al., 2013).

RCP8.5 may be becoming increasingly unlikely due to the overestimation of future coal use (Ritchie & Dowlatabadi, 2017; Schwalm et al., 2020), but it remains valuable especially for mid-century projections, to assess policies or to account for higher-than-expected carbon cycle feedbacks (Schwalm et al., 2020).

Road weather observations

We collected observations of road surface temperature and road surface conditions from representative road weather stations in Finland (25 stations, 2002–2005), Sweden (5 stations, 2015–2018) and Norway (5 stations, 2015–2018) in hourly resolution (see details in Online Resource T1). Three of the Norwegian stations are located in mountainous regions near or above 1000-m elevation, which brings challenges to model evaluation as the terrain differences between the model and observations can be large. Swedish observations were from around the country, with one on a bridge. The Finnish observations were more numerous, because there were more reliable observation data available, and the same list of stations was used in the previous study by Toivonen et al. (2019).

Finnish road weather stations use the Vaisala ROSA road weather package equipped with asphalt-embedded DRS511 sensors. Swedish observation data was provided by the PT-100 resistance thermometer probe (Platina 100) embedded in the road and a DSC111 optical sensor (Vaisala). The Norwegian observations were recorded with weather stations from Scanmatic (sensors not communicated).

For the evaluation, we selected the modelled grid cell closest to the stations' coordinates. Thus, the observations were point measurements, whilst the modelled data were an average over one grid cell.

Methods

Henceforth, RoadSurf runs driven with ECE-HCLIM38-ALADIN and GFDL-HCLIM38-ALADIN will be referred to as ECE–driven and GFDL–driven runs, respectively.

Evaluation against observations

We compared historical RoadSurf simulations to the road weather observations in FNS for the years 2002–2005 to assess RoadSurf's predictive accuracy when driven with different combinations of HCLIM38 configurations (-ALADIN or -AROME) and global climate models (ECE or GFDL) as well as with ERAI reanalysis data.

Probability density functions (PDFs) of the regionally observed road surface temperatures (T_{RS}) were compared to HCLIM38-ALADIN simulations (ERAI, ECE-historical, GFDL-historical) over FNS. Norwegian and Swedish observations did not overlap with the modelled years, so we compared 2015–2018 with the years 2002–2005 from the model under the assumption that the climate did not considerably change during the gap. Thereafter, we calculated the monthly mean bias (MMB, model minus observations) and mean absolute error (MAE) of the modelled T_{RS}.

Road surface condition observations were only available for Finland and Sweden. We compared the observed time fractions of the occurrence of each road surface condition to HCLIM38-ALADIN runs (ERAI, ECE-historical, GFDL-historical). Road surface conditions in historical simulations in Norway were only compared to their corresponding ERAI run.

Modelled traffic and pedestrian indices could not be evaluated against observations as no such observation data existed to our best knowledge. However, we compared the historical simulations with the ERAI-HCLIM38-ALADIN runs.

Furthermore, we assessed whether there was an additional value of using the computationally heavier high-resolution HCLIM38-AROME configuration over HCLIM38-ALADIN in terms of road weather predictions with RoadSurf (three-fold longer run time with four-fold storage space needed for RoadSurf simulation with HCLIM38-AROME data) by repeating all abovementioned evaluation steps for HCLIM38-AROME and comparing them to HCLIM38-ALADIN and observations.

Projected future driving and walking conditions

We analysed T_{RS}, driving conditions, road surface conditions, pedestrian conditions and zero-degree-crossing (ZDC) days for their temporal development and change in

the mid-century (2041–2060) and end-century (2081–2100) compared to the historical period (1986–2005) in the northern and southern parts of FNS. Traffic and pedestrian conditions depict the level of hazard due to road or walkway slipperiness and weather.

To analyse the changes in occurrence of road surface conditions, we counted the average seasonal time fraction for each condition (dry, damp, wet, snow, frost, icy, partly icy) and compared mid-century and end-century results to the historical period, as well as ECE-RoadSurf and GFDL-RoadSurf results against each other. For further analysis, we also assessed the spatial distributions of the changes.

We repeated the same analysis for the driving conditions (normal, difficult, very difficult) and pedestrian conditions (normal, slippery, very slippery I, II and III). The driving condition "very difficult" occurs rarely and only for short periods during extreme weather events, such as heavy snowfall. For this reason, the "difficult" and "very difficult" driving categories were grouped into one.

ZDC-days give valuable information as most traffic accidents happen when T_{RS} is close to 0 °C (Andersson & Chapman, 2011a). We defined a ZDC-day as a day on which the T_{RS} (at least once) drops from above + 0.5 °C to below − 0.5 °C (or vice versa) causing freezing of water (or melting of ice and snow) on the road surface. We calculated monthly averages of ZDC-days. Subsequently, we calculated the change in average seasonal ZDC-days over the century compared to the historical period and performed a Student's *t*-test. We also compared the PDFs of historical and future ZDC-days estimates between GFDL-RoadSurf and ECE-RoadSurf.

Results

Evaluation against observations

We compared T_{RS}, PDFs, MMB and MAE of HCLIM38-ALADIN-RoadSurf and HCLIM38-AROME-RoadSurf driven by the ERAI reanalysis data to observations in FNS to quantify if the higher horizontal resolution of HCLIM38-AROME configuration brought benefits over HCLIM38-ALADIN when used as an input in RoadSurf. Means, temporal variation and seasonal patterns of modelled road surface temperature (T_{RS}) and road surface conditions agreed well with observations in Finland, Norway and Sweden (FNS).

The PDFs showed that both HCLIM38 configurations reproduced observations almost interchangeably well, with a small exception for spring in Finnish Lapland, where HCLIM38-AROME estimated stronger variability around 0 °C than observed (not shown).

The MAE showed that both HCLIM38 configurations reproduced observed T_{RS} accurately over flat inland regions. For Norway however, both HCLIM38 configurations became increasingly inaccurate. In the Norwegian mountains and northern Norwegian Fjords, HCLIM38-AROME showed better results. This may be attributed to the fact that HCLIM38-AROME can resolve topography-related features better than HCLIM38-ALADIN. However, considering all the above results, the improvement was not deemed sufficient to warrant the use of computationally more expensive HCLIM38-AROME simulations for the climate change analysis.

HCLIM38-ALADIN-RoadSurf driven by three different boundary data, the ERAI, ECE-historical and GFDL-historical, reproduced T_{RS} observations satisfyingly over Finland, but produced slightly lower autumn- and wintertime T_{RS} compared to observations in Sweden and Norway (Fig. 1). The inaccuracy in the simulated wintertime T_{RS} over Norway might stem from topography inaccuracies on the one hand, and sensors submerged in snow on the other. However, due to the lack of information which sensors were used (optical or asphalt-embedded, etc.), it is difficult to estimate the root cause for the negative bias.

ECE- and GFDL-RoadSurf both overestimated the occurrence of icy road surfaces whilst grossly underestimating frost (Online Resource F1a). Overestimation of icy surfaces was acceptable for the original near future (0–24 h) warning purposes of the model, but must be kept in mind when interpreting the future results in this study. GFDL-RoadSurf yielded more extreme under- and overestimations than ECE-RoadSurf.

The ECE- and GFDL-RoadSurf driving conditions agreed very well with the ERAI reanalysis (Online Resource F1b). GFDL-RoadSurf produced overall more frequent occurrence of difficult driving conditions, with the largest model differences in Finnish Lapland.

Despite the small discrepancies between the modelled and observed road weather parameters, we concluded that the overall performance of RoadSurf was satisfying for this study.

Projected future driving and walking conditions

Road surface temperature

We calculated the whole-period mean of T_{RS} for the historical period (1986–2005), mid-century (2041–2060) and end-century (2081–2100). Both ECE-RoadSurf and GFDL-RoadSurf estimated a clear increase in T_{RS} for all parts of FNS (Fig. 2). Whilst 46.9%/43.5% (ECE-RoadSurf/GFDL-RoadSurf) of historical monthly T_{RS} means over the whole domain were below 0 °C, in the mid-century this dropped to 39.8%/36.4% and even further to only 29.7%/23.9% in the end-century period.

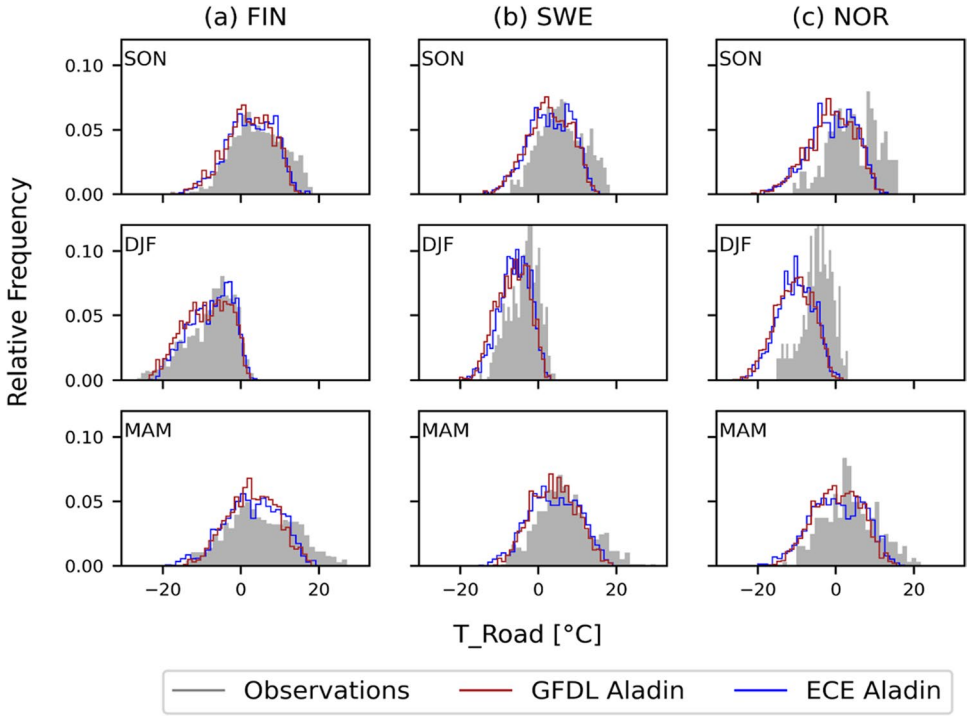

Fig. 1 Comparison of daily road surface temperature observations and simulations for **a** Finland (FIN, left column), **b** Sweden (SWE, middle column) and **c** Norway (NOR, right column) in autumn (September–October–November; SON, top row), winter (December–January–February; DJF, middle row) and spring (March–April–May; MAM, bottom row) driven by ECE-HCLIM38-ALADIN (ECE Aladin) and GFDL-HCLIM38-ALADIN (GFDL Aladin). The simulations covered the historical period 2002–2005 and the observations covered 2002–2005 over Finland and 2015–2018 over Sweden and Norway

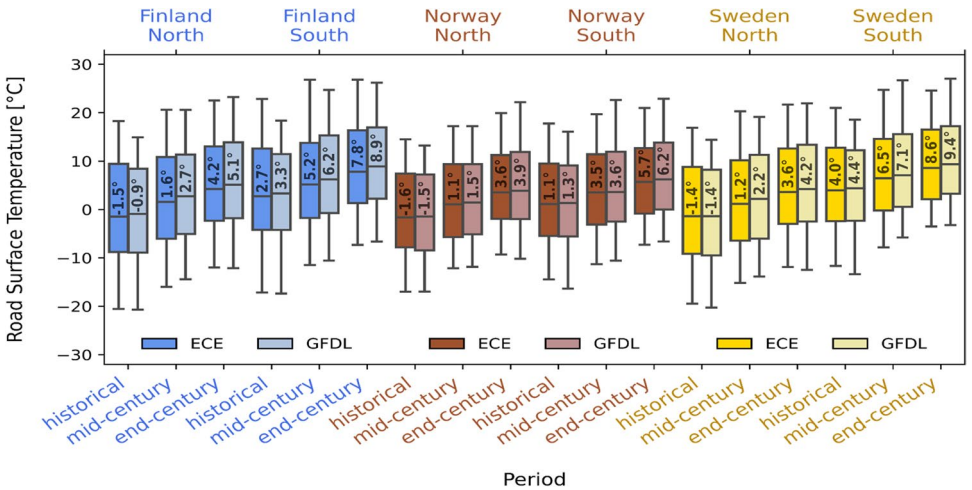

Fig. 2 Average regional road surface temperatures over the whole historical (1986–2005), mid-century (2041–2060) and end-century (2081–2100) periods in the northern and southern halves of Finland (blue), Norway (brown) and Sweden (yellow). The boxes enclose the first and third quartile. The numbers inside the boxes represent the region's median road surface temperature in the given period in °C. The whiskers represent the minimum and maximum simulated temperatures simulated by ECE-HCLIM38-ALADIN-RoadSurf (ECE, dark shades) and GFDL-HCLIM38-ALADIN-RoadSurf (GFDL, light shades) following the RCP8.5 scenario

During autumn (September to November, SON), T_{RS} increased 2.5 °C/3.7 °C on average in the mid-century period and 4.9 °C/6.8 °C in the end-century, compared to historical values (Fig. 3 and Online Resource F3). A slight north–south gradient in T_{RS} increase was simulated to intensify over the course of the century for autumn as well.

The strongest T_{RS} warming was simulated for meteorological winters (December to February, DJF), with an average increase of 2.7 °C/3.9 °C in the mid-century and a 6.2 °C/7.2 °C increase in the end-century.

GFDL-RoadSurf simulations showed an extreme T_{RS} increase of > 4.5 °C regionally in Finland (especially south-eastern Finland) during the mid-century, which intensified and extended into the Norwegian mountain range and its entire piedmont with > 8 °C increase in the end-century period.

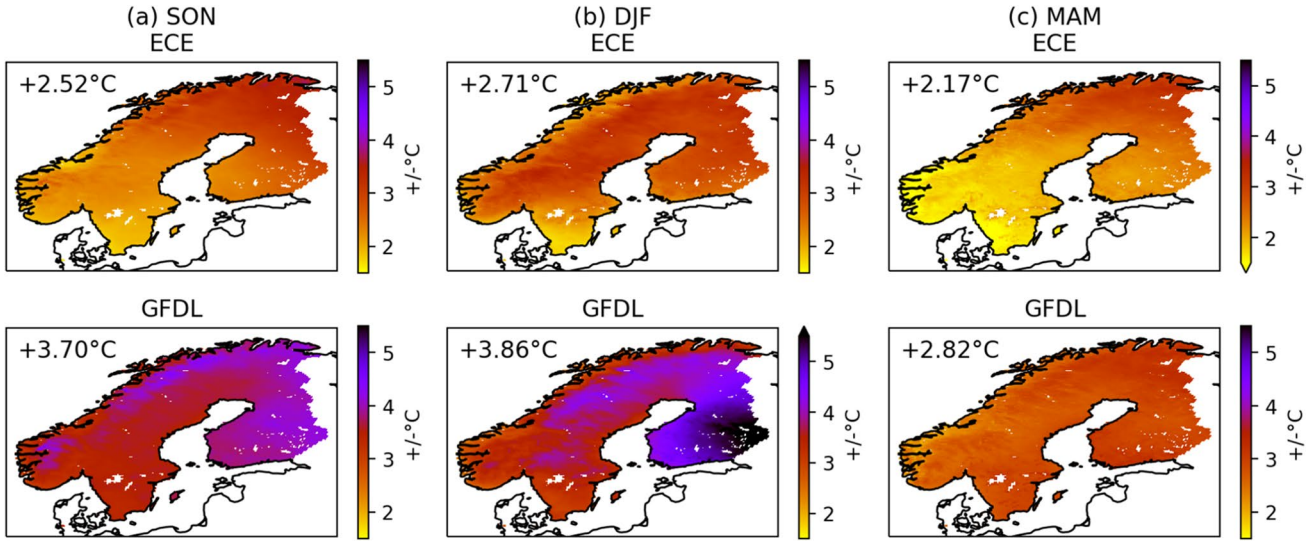

Fig. 3 Projected seasonal road surface temperature change in Finland, Norway and Sweden in the mid-century period (2041–2060) compared to the historical period (1986–2005) **a** autumn (SON, left column), **b** winter (DJF, middle column) and **c** spring (MAM, right column), as estimated by ECE-HCLIM38-ALADIN-RoadSurf (ECE, top row) and GFDL-HCLIM38-ALADIN-RoadSurf (GFDL, bottom row) in the RCP8.5 scenario. Displayed in the top left corners are the road surface temperature changes averaged over the whole region for the corresponding season (for the end-century see Online Resource F3)

ECE-RoadSurf, on the other hand, simulated an almost uniform T_{RS} increase across the three countries in mid-century winter, except for weaker T_{RS} increase in the southern tip of Sweden. A strong acceleration in T_{RS} warming occurred in end-century with > 7.5 °C regional T_{RS} increase in the northern parts of FNS. This roughly agreed with the estimated warming from the GFDL-RoadSurf simulations.

Springtime T_{RS} values (March to May, MAM) warmed 2.2 °C/2.8 °C in the mid-century and 4.6 °C/5.0 °C in the end-century. Whilst GFDL-RoadSurf showed a spatially uniform T_{RS} increase, ECE-RoadSurf estimated a noticeably weaker T_{RS} warming for southern Norway and Sweden, with partially < 1.5 °C T_{RS} increase (compared to > 2.5 °C in more northern latitudes) in the mid-century and < 4 °C (compared to > 5 °C in more northern latitudes) in the end-century period during spring.

Road surface conditions

We calculated the change in occurrence of road surface conditions (dry, damp, wet, snow, frost, icy, partly icy) in the mid-century and end-century compared to the historical period.

The simulations for the cold season from September to May showed an overall decline in snowy and icy road surfaces with up to 17.3/23.0 percentage points (PPs) less in the mid-century and up to 39.6/47.0 PPs less in the end-century (Fig. 4). Autumn and spring showed large changes during the mid-century and a decelerated change until the end-century. The strongest changes were indicated for autumn with a combined average decrease of 9.5/14.7 PPs in snow and ice storages on roads in the mid-century and a decrease of 17.4/22.5 PPs in the end-century. Hence, dry roads were simulated to be 7.7/10.1 PPs more frequent in mid-century autumn and 13.4/15.6 PPs more frequent in end-century autumn, compared to historical ones. Spring showed 3.0/4.4 PPs more frequent dry road surface conditions for mid-century and 7.5/7.0 PPs more frequent for end-century.

The net change in the occurrence of road surface conditions in DJF in Fig. 4 seems to be small compared to the change seen in SON, especially in the mid-century, which might leave the illusion that mid-century winters were simulated to expect as much snow and ice on roads as in the historical period. Further investigation however showed that the small net change was attributed to strongly contrasting, region-dependent developments.

Whilst northern parts of FNS showed a 1–9/9–15 PPs shift towards icy road surface conditions in winter, southern Finland and the southern tip of Sweden showed a 3–11/0–21 PPs increase in dry winter road surface conditions. Snowy road surfaces in the Norwegian mountain range, central Sweden and elevated parts of Lapland increased by up to 6.4/6.4 PPs in the mid-century estimates, but decreased by the same amount for southern Sweden, southern Finland and the Norwegian fjords. In autumn and spring, almost all regions showed drier road surface conditions, possibly due to earlier snow melt, except for the glacial regions of Norway, where the earlier onset of spring caused an increase of 0–5/0–5 PPs in wet road surface conditions as well as slight increases

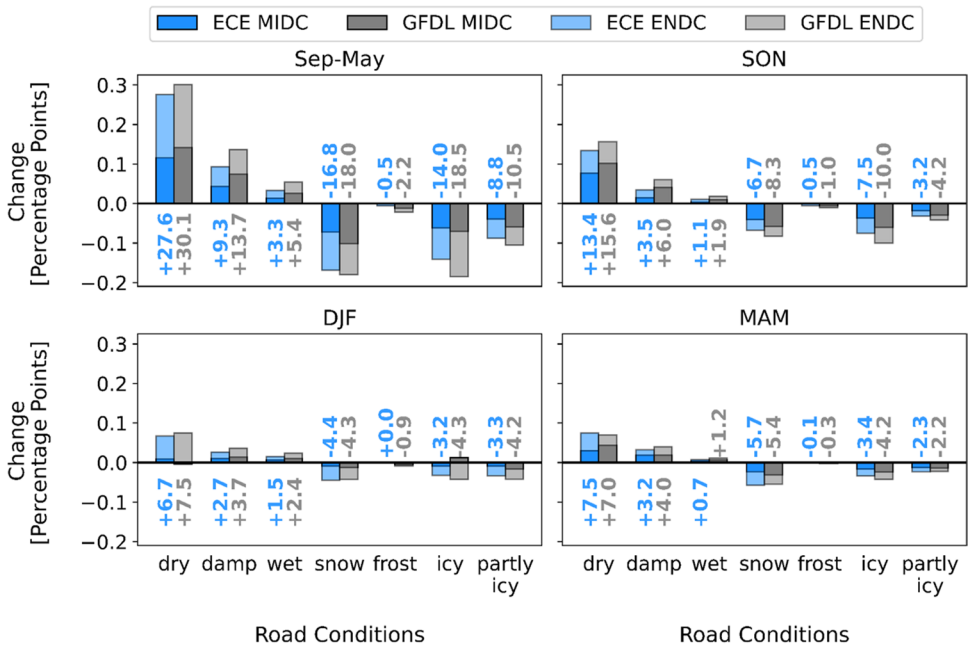

Fig. 4 Projected changes in occurrences of road surface conditions in the cold season from September to May (September until May), autumn (SON), winter (DJF) and spring (MAM) during mid-century (MIDC, 2041–2060, dark bars) and end-century (ENDC, 2081–2100, light bars) compared to the historical period (1986–2005) in Finland, Norway and Sweden as estimated by ECE-HCLIM38-ALADIN-RoadSurf (ECE, blue bars) and GFDL-HCLIM38-ALADIN-RoadSurf (GFDL, grey bars) under the RCP8.5 scenario. The bar labels show the resulting change by the end of the century compared to the historical period in gained or lost percentage points

Table 2 Average historic ratio of road surface conditions (HIST) in percent and change in road surface condition occurrences for the mid-century (MIDC) and end-century (ENDC) in percentage points compared to the historic period in the northern and southern halves of Finland, Norway and Sweden. Results are shown in the format "ECE-RoadSurf estimates/GFDL-RoadSurf estimates" with increases in green and decreases in red

Region	Period	dry [±PPs]	damp [±PPs]	wet [±PPs]	snow [±PPs]	frost [±PPs]	icy [±PPs]	partly icy [±PPs]
Finland North	HIST	57.9% / 54.8%	3.6% / 3.9%	0.7% / 0.9%	9.7% / 11.1%	1.7% / 1.5%	16.6% / 17.6%	7.0% / 7.4%
	MIDC	+2.2 / +3.2	+0.8 / +1.5	+0.3 / +0.5	-1.5 / -2.5	0.0 / -0.4	-0.7 / -0.6	-1.1 / -1.8
	ENDC	+6.1 / +6.6	+1.8 / +2.9	+0.7 / +1.2	-3.4 / -3.9	**-0.2 / -0.6**	-2.6 / -3.0	-2.4 / -3.2
Finland South	HIST	63.1% / 60.9%	4.8% / 5.1%	1.2% / 1.4%	7.7% / 8.1%	1.4% / 1.4%	13.4% / 14.8%	5.2% / 5.2%
	MIDC	+ 3.9 / +4.0	+0.9 / +1.9	+0.2 / +0.6	-1.8 / -2.1	0.0 / -0.4	-1.8 / -2.3	-1.4 / -1.7
	ENDC	**+9.5 / +9.6**	+1.9 / +3.6	+0.6 / +1.1	-3.9 / -4.2	**-0.2 / -0.6**	**-5.0 / -6.3**	**-2.9 / -3.2**
Norway North	HIST	51.7% / 48.1%	5.0% / 4.0%	1.4% / 1.1%	15.6% / 17.1%	1.2% / 1.4%	14.3% / 17.2%	6.4% / 7.1%
	MIDC	+3.2 / +2.5	+1.6 / +2.3	+0.7 / +0.9	-3.7 / -3.9	+0.2 / -0.2	-0.7 / -0.4	-1.2 / -1.3
	ENDC	+6.6 / +4.9	**+4.2 / +4.6**	**+1.8 / +2.0**	**-7.5 / -6.4**	+0.1 / -0.4	-2.7 / -2.2	-2.5 / -2.5
Norway South	HIST	57.2% / 53.8%	6.4% / 6.4%	2.4% / 2.5%	12.8% / 14.6%	1.5% / 1.2%	12.4% / 13.3%	4.9% / 5.3%
	MIDC	+2.2 / +2.3	+1.3 / +2.6	+0.7 / +1.4	-1.9 / -3.5	-0.1 / -0.2	-1.6 / -1.5	-0.7 / -1.1
	ENDC	+4.5 / +5.1	+2.7 / +4.3	**+1.5 / +2.6**	-4.5 / -5.9	-0.2 / -0.4	-2.4 / -3.7	-1.6 / -2.0
Sweden North	HIST	55.5% / 51.1%	3.7% / 3.5%	0.7% / 0.8%	11.3% / 13.8%	1.9% / 1.7%	17.6% / 18.3%	6.3% / 7.2%
	MIDC	+1.9 / +2.4	+0.7 / +1.4	+0.3 / +0.5	-1.2 / -2.1	0.0 / -0.3	-1.1 / -0.6	-0.6 / -1.4
	ENDC	+4.7 / +4.4	+1.7 / +2.9	+0.8 / +1.3	-3.2 / -3.5	-0.1 / -0.5	-2.1 / -2.2	-1.7 / -2.3
Sweden South	HIST	67.6% / 62.8%	5.3% / 5.4%	1.4% / 1.5%	6.3% / 8.0%	1.7% / 1.4%	12.4% / 14.6%	3.3% / 4.2%
	MIDC	+3.9 / +5.0	+0.9 / +1.7	+0.1 / +0.5	-1.5 / -2.5	-0.1 / -0.3	-2.5 / -2.9	-0.8 / -1.4
	ENDC	**+8.2 / +9.9**	+1.6 / +2.5	+0.4 / +0.9	-3.5 / -4.2	-0.2 / -0.5	-4.6 / -6.1	-1.9 / -2.5

(< 5 PPs) in icy and partly icy road surface conditions in the mid-century, which is most probably connected to the simultaneous increase in ZDC days (see section "Zero-degree-crossing days") in these regions. Changes in road surface condition occurrences of the regions are listed in Table 2.

Driving conditions

We calculated the change in driving condition occurrences (normal, difficult, very difficult) from historical to mid- and end-century.

"Normal" driving conditions increased strongly in all parts of FNS. The mid-century cold season (September until May) showed a 12.2/18.5 PP increase of normal driving conditions, which increased to + 28.5/33.2 PPs for the end-century compared to the historical period (Fig. 5a). The strongest increase of easier driving conditions was seen in autumn with + 6.3/9.8 PPs in the mid-century and + 11.2/14.3 PPs by the end-century, followed by spring with + 3.7/5.0 PPs in the mid-century and + 8.6/8.6 PPs in the end-century.

Winter showed a moderate change at first with only + 2.2/3.6 PPs in mid-century, but a strong acceleration of change for end-century with an + 8.7/10.3 PPs increase in normal driving conditions.

ECE-RoadSurf simulated the strongest increases in normal driving conditions along the Norwegian coasts and the southern half of Finland (Fig. 5b and Online Resource F4). GFDL-RoadSurf estimated an overall stronger change with the largest changes in southern Norway, southern Finnish Lapland and the valleys of the Scandinavian mountains.

Pedestrian conditions

We calculated the occurrence of pedestrian conditions normal, slippery and very slippery (VS) I, II and III in the historical, mid-century and end-century periods.

The projected walking conditions showed strong seasonality as well as regional differences. Generally, in the cold season between September and May, the pedestrian condition "slippery" was estimated to decrease by 7.0/8.5 PPs in the mid-century and 18.4/18.4 PPs in the end-century, compared to the historical period. An increase was simulated for "normal" (+ 4.9/5.0 PPs mid-century and + 17.7/11.8 PPs end-century) and "VS II" (+ 3.9/5.3 PPs mid-century and + 6.9/11.8 PPs end-century) (Fig. 6).

Similarly, to the changes in driving conditions, the strongest changes in pedestrian conditions were seen for autumn, during which "normal" walking conditions increased by an average 7.8/11.5 PPs for mid-century and 14.3/17.5 PPs for end-century. The most strongly affected regions were the Norwegian fjords and the piedmont of the Scandinavian mountains (Online Resource F6). Estimates for winter showed a clear shift from "normal" conditions towards "slippery" pedestrian indices with the strongest increase in "VS II" (+ 2.9/4.1 PPs in mid-century and + 6.8/10.6 PPs in end-century).

Almost all regions show this increase, except for the southern tip of Sweden and in the south-western coastline of Norway, where the "slippery" indices decreased. Spring

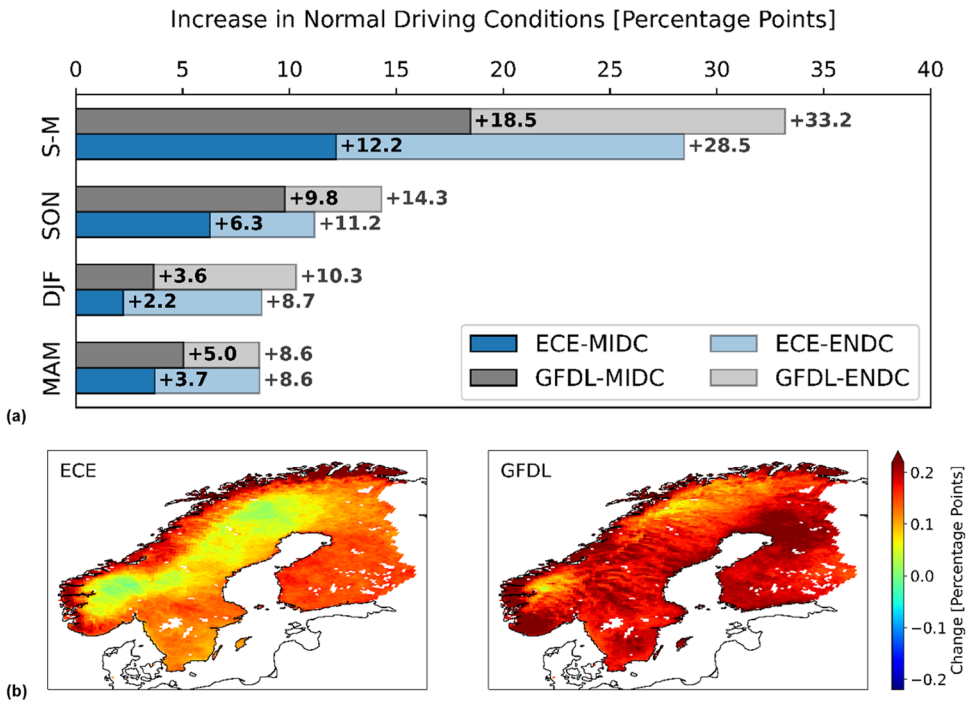

Fig. 5 **a** Increase in "normal" (less dangerous) driving conditions in percentage points for autumn (SON), winter (DJF) and spring (MAM) and the cold season from September to May (S-M) in the mid-century (MIDC, 2041–2060, dark bars) and end-century (ENDC, 2081–2100, light bars) compared to the historical period (1986–2005) in Finland, Norway and Sweden. **b** Changes in "normal" driving conditions during the mid-century cold season from Septemeber to May (275 days in total) compared to the historical period in Finland, Norway and Sweden (for the end-century see Online Resource F4). Estimates by ECE-HCLIM38-ALADIN-RoadSurf (ECE, **a** blue bars/**b** left side) and GFDL-HCLIM38-ALADIN-RoadSurf (GFDL **a** grey bars/**b** right side) with the RCP8.5 scenario

showed a slight increase in "VS II" condition too, with a 1.0/1.8 PP increase for mid-century and 1.1/3.0 PP increase for end-century. However, the "normal" condition increased simultaneously by 1.6/2.6 PPs mid-century and 7.0/4.8 PPs end-century. These changes affected mostly the Norwegian fjords and the Scandinavian mountain range.

Zero-degree-crossing days

We calculated the seasonal average number of ZDC-days, i.e. days when T_{RS} decreased from minimum + 0.5 °C to − 0.5 °C (or vice versa). ECE-RoadSurf and GFDL-RoadSurf estimated a mostly steady increase in winter ZDC-days and decrease in autumn and spring (attributed to the later onset and earlier end of cold winter temperatures), however with strong regional differences (Fig. 7).

Regions above the Arctic Circle and around the Norwegian mountain range showed minor changes (max. ± 2 ZDC-days) in all seasons during the mid-century (Fig. 7). Finnish regions south of the Arctic Circle showed 2–3/3–6 additional ZDC-days on average in mid-century winter, with the strongest increase in south and south-west Finland. The same regions showed an estimated decrease of 2–4/4–5 ZDC-days in autumn and a decrease of 1–5/3–7 ZDC-days in spring.

Other considerable changes in mid-century ZDC-days were simulated for the Norwegian fjords, southern Sweden and Swedish regions around the Bothnian sea. Mid-century winters showed 1–4/0–1 fewer ZDC-days to regions around the Kattegat strait and 3–5/4–6 more ZDC-days to regions around the Bothnian sea. Autumns of southern Sweden and the Norwegian fjords showed 3–5/3–5 fewer ZDC-days, whilst spring showed 2–5/4–8 more ZDC-days compared to the historical period.

The number of ZDC-days increased even more in wintertime by the end of the century (Online Resource F7). End-century simulations for regions north of the Arctic Circle showed 1–5/2–5 more wintertime ZDC-days, as well as 0–3/1–4 fewer autumn and 0–4/0–5 fewer spring ZDC-days. An increase of 4–10/4–10 wintertime ZDC-days was simulated for almost all regions in FNS below the Arctic Circle (with exception of the southern tip of Sweden with 0–5/0–5 fewer winter ZDC-days). The same regions showed 3–6/4–7 fewer autumn and 3–8/5–13 fewer spring ZDC-days.

The Student's *t*-test concluded all the above shown results of changes in ZDC-days to be statistically significant on a 5% level compared to the historical ZDC-days.

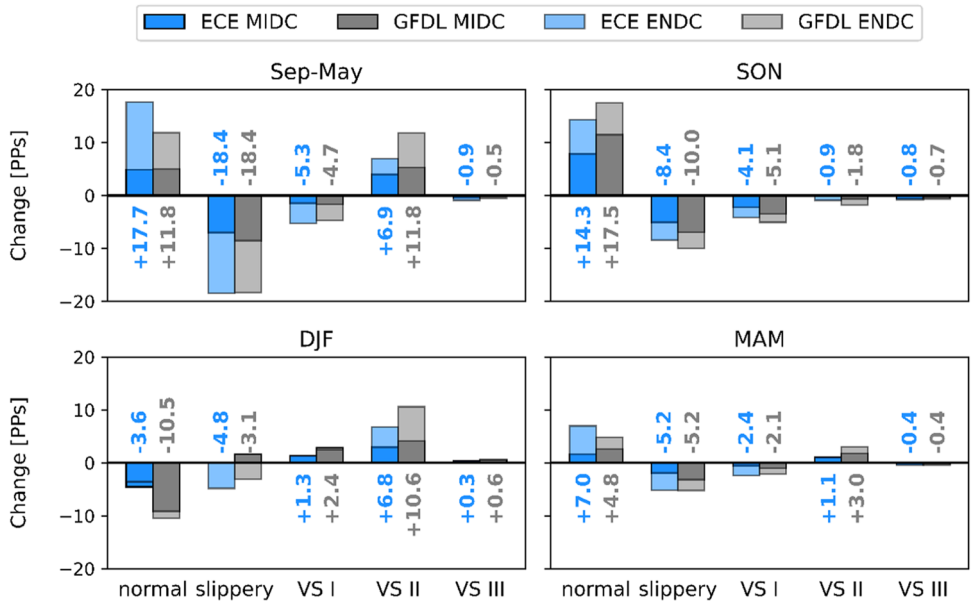

Fig. 6 Projected changes in the occurrences of pedestrian conditions (in percentage points (PPs)) in the cold season from September to May (Sep–May), autumn (SON), winter (DJF) and spring (MAM) during mid-century (MIDC, 2041–2060) and end-century (ENDC, 2081–2100) compared to the historical period (1986–2005) in Finland, Norway and Sweden as estimated by ECE-HCLIM38-ALADIN-RoadSurf (ECE, blue bars) and GFDL-HCLIM38-ALADIN-RoadSurf (GFDL, grey bars) in the RCP8.5 scenario for the pedestrian indices normal, slippery, very slippery due to foot-packed snow (VS I), very slippery due to water above ice layer (VS II) and very slippery due to snow above ice layer (VS III) over the whole domain, where the bar labels show the resulting change by the end of the century compared to the historical period (for the map view see Online Resource F6)

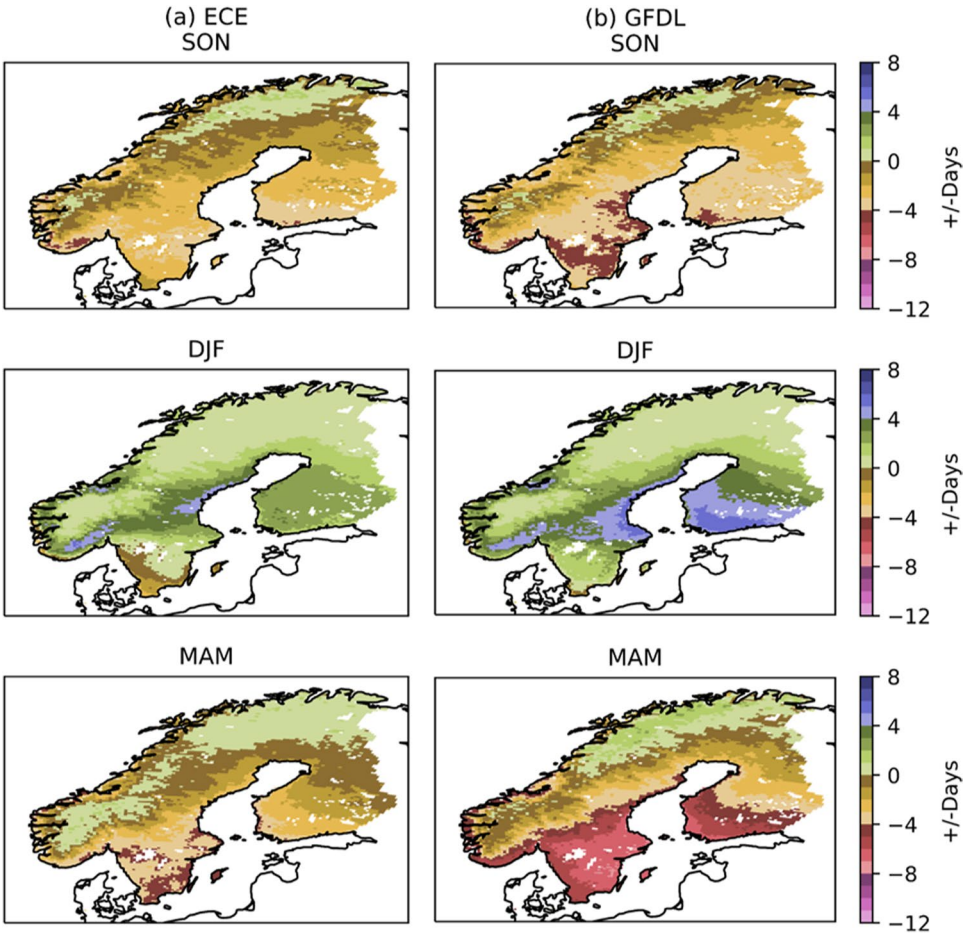

Fig. 7 Change in the average seasonal number of zero-degree-crossing days in the mid-century (2041–2060) compared to the historical period (1986–2005) during autumn (SON, top row), winter (DJF, middle row) and spring (MAM, bottom row) estimated by **a** ECE-HCLIM38-ALADIN-RoadSurf (ECE, left column) and **b** GFDL-HCLIM38-ALADIN-RoadSurf (GFDL, right column) under the RCP8.5 scenario. For the end-century (2081–2100) results see Online Resource F7

Discussion and conclusions

In this study, we assessed the climate change impacts on driving and walking conditions in Finland, Norway and Sweden (FNS) based on simulations carried out with FMI's road weather model RoadSurf driven by ECE-HCLIM38-ALADIN and GFDL-HCLIM38-ALADIN (ECE-RoadSurf and GFDL-RoadSurf, respectively). Our results are based on the RCP8.5 scenario, a worst-case climate change scenario that anticipates an unprecedented increase in greenhouse gas emissions. Therefore, our simulations are upper extreme estimates, but can serve as a reference of locality and seasonality of the expected changes, and thus help local decision-makers to plan for mitigation and adaptation measures ahead of time.

We concluded that the model performance was accurate enough to carry out the climate change projections for this study, albeit RoadSurf was shown to overestimate dry and icy road surface conditions. The considerably lower computational expense of the HCLIM38-ALADIN configuration allows a wider set of modelled road weather scenarios and is generally preferable, however at the cost of losing topographical features compared to the HCLIM38-AROME configuration, which should be considered for studying regions with large elevation differences.

Our simulations suggested a strong increase in the average annual road surface temperatures (T_{RS}), with the strongest regional T_{RS} increases in southern Finland and southern Sweden. Winters showed an increase in water above ice on walkways (except for the southern tip of Sweden). Autumn and spring, however, showed a decrease in slippery pedestrian conditions. Hence, the future pedestrian slip-injury season might be shorter, mostly confined to winter, but with an exacerbated risk for slipping. Zero-degree-crossing days (ZDCs-days) were estimated to decrease in autumn and spring (apart from an increase north of the Arctic Circle), but to increase in winter. An increasing number of ZDC-days is a major hazard for pedestrians, as temperatures near 0 °C pose one of the greatest risks for pedestrian slip accidents (Hippi et al., 2020).

The results also showed a decrease in snowy, frosty and icy road surface conditions and an increase in dry, damp and wet road surface conditions. As a result, there was a strong decrease in difficult driving conditions during the cold season between September and May.

This is congruent with studies of countries with comparable climates like Canada, where 43% less slippery-related accidents and less road maintenance costs were estimated due to the easier driving conditions (Andersson & Chapman, 2011b). Intuitively, one could expect less traffic accidents due

to slippery roads based on our results (Norrman et al., 2000). However, in different studies, the number of accidents did not change in less slippery road conditions, as they evened out with drivers paying less attention in less dangerous driving conditions (Andersson & Chapman, 2011a; Bernard et al., 2001). The combination of more frequently wet roads and more ZDC-occurrences observed in our study could still be exacerbating the risk for traffic accidents, as slippery conditions near 0 °C might be less apparent to drivers (than e.g. snow-covered roads); thereby, drivers could be at risk of underestimating the immediate slip risk and not adjust their level of attention.

As climate change progresses, it is important to understand and be ready for the changes to come. Our results motivate us to recommend road managers and authorities in Nordic countries—amongst others, Destia, Traficom and Fintraffic in Finland, Trafikverket in Sweden and Statens vegvesen in Norway—to plan actions and secure necessary budgets for managing the shorter, but more intense, slippery roads and walkways in the future successfully.

Supplementary Information The online version contains supplementary material available at https://doi.org/10.1007/s10113-022-01920-4.

Acknowledgements This work was supported by the Academy of Finland (grant number: 329241) and the Maj and Tor Nessling foundation. The HCLIM simulations were performed by the NorCP (Nordic Convection Permitting Climate Projections) project group. The HCLIM simulations were partly funded by the European Climate Prediction System project (EU Horizon 2020; Grant no. 776613). We acknowledge the storage resource Bi provided by the Swedish National Infrastructure for Computing (SNIC) at the Swedish National Supercomputing Centre (NSC) at Linköping University. Furthermore, the lead author would like to express her thanks to Prof. Tommi Ekholm for his support in the writing process.

Data availability The data analysed in this paper can be accessed through the https://doi.org/10.23728/fmi-b2share.8be17e3ebccf4fff869fd5ddaab7361d.

References

Andersson A, Chapman L (2011a) The use of a temporal analogue to predict future traffic accidents and winter road conditions in Sweden. Meteorol Appl. https://doi.org/10.1002/met.186

Andersson A, Chapman L (2011b) The impact of climate change on winter road maintenance and traffic accidents in West Midlands UK. Accid Anal Prev 43(1):284–289. https://doi.org/10.1016/j.aap.2010.08.025

Axelsen C, Grauert M, Liljegren E, Bowe M, Sladek B (2016) Implementing climate change adaptation for european road administrations. Transp Res Procedia 14:51–57. https://doi.org/10.1016/j.trpro.2016.05.040

Balston J, Li S, Iankov I, Kellett J, Wells G (2017) Quantifying the financial impact of climate change on Australian local government roads. Infrastructures. https://doi.org/10.3390/infrastructures2010002

Belušić D, De Vries H, Dobler A, Landgren O, Lind P et al (2020) HCLIM38: a flexible regional climate model applicable for different climate zones from coarse to convection-permitting scales. Geosci Model Dev 13(3):1311–1333. https://doi.org/10.5194/GMD-13-1311-2020

Bengtsson L, Andrae U, Aspelien T, Batrak Y, Calvo J et al (2017) The HARMONIE-AROME model configuration in the ALADIN-HIRLAM NWP system. Mon Weather Rev 145(5):1919–1935. https://doi.org/10.1175/MWR-D-16-0417.1

Bernard A, Bussière YD, Thouez JP (2001) A comparison between winter and summer road traffic accidents in Quebec between 1989 and 1996. In Recherche - Transports - Sécurité (73 41–42). https://doi.org/10.1016/s0761-8980(01)90038-x

Chapman L, Thornes JE, Bradley AV (2001) Modelling of road surface temperature from a geographical parameter database. Part 2: Numerical. Meteorological Applications 8(4):421–436. https://doi.org/10.1017/S1350482701004042

Crevier L-P, Delage Y (2001) METRo: a new model for road-condition forecasting in Canada. J Appl Meteorol 40:2026–2037. https://doi.org/10.1175/1520-0450(2001)040%3c2026:MANMFR%3e2.0.CO;2

Dee D, Uppala SM, Simmons AJ, Berrisford P, Poli P et al (2011) The ERA-interim reanalysis: configuration and performance of the data assimilation system. Q.J.R Meteorol Soc 137:553–597

Donner LJ, Wyman BL, Hemler RS, Horowitz LW, Ming Y et al (2011) The dynamical core, physical parameterizations, and basic simulation characteristics of the atmospheric component AM3 of the GFDL global coupled model CM3. J Clim 24(13):3484–3519. https://doi.org/10.1175/2011JCLI3955.1

Elvik R, Bjørnskau T (2019) Risk of pedestrian falls in Oslo, Norway: relation to age, gender and walking surface condition. In Journal of Transport & Health (12 359–370). https://doi.org/10.1016/j.jth.2018.12.006

Elvik R, Vaa T, Hoye A, Sorensen M (2009) *The handbook of road safety measures: second edition*. Emerald Group Publishing. https://books.google.com/books/about/The_Handbook_of_Road_Safety_Measures.html?hl=&id=JuTAZmIseeACLB-LOKz

European Commission Directorate-General for Mobility and Transport, & CE Delft (2019). *Handbook on the external costs of transport* (H. van Essen, D. Fiorello, K. El Beyrouty, C. Bieler, L. van Wijngaarden, A. Schroten, R. Parolin, M. Brambilla, D. Sutter, S. Maffii, & F. Fermi (eds.); 3rd ed.). Publications Office of the European Union. https://doi.org/10.2832/51388

Forzieri G, Bianchi A, Silva FBE, Marin Herrera MA, Leblois A et al (2018) Escalating impacts of climate extremes on critical infrastructures in Europe. Glob Environ Chang 48:97–107. https://doi.org/10.1016/j.gloenvcha.2017.11.007

Fujimoto A, Saida A, Fukuhara T (2012) A new approach to modeling vehicle-induced heat and its thermal effects on road surface temperature. J Appl Meteorol Climatol 51:1980–1993. https://doi.org/10.1175/JAMC-D-11-0156.1

Griffies S, Winton M, Donner L, Horowitz L, Downes S et al (2011) The GFDL CM3 coupled climate model: characteristics of the ocean and sea ice simulations. J Clim 24:3520–3544. https://doi.org/10.1175/2011JCLI3964.1

Hazeleger W, Severijns C, Semmler T, Stefanescu S, Yang S et al (2010) EC-Earth: a seamless Earth-system prediction approach in action. Bull Am Meteor Soc 91(10):1357–1364. https://doi.org/10.1175/2010BAMS2877.1

Hazeleger W, Wang X, Severijns C, Briceag S, Bintanja R et al (2011) EC-Earth V2.2: description and validation of a new seamless Earth system prediction model. Clim Dyn 39:1–19. https://doi.org/10.1007/s00382-011-1228-5

Hippi M, Kangas M, Ruuhela R, Ruotsalainen J, Hartonen S (2020) RoadSurf-pedestrian: a sidewalk condition model to predict risk for wintertime slipping injuries. In Meteorological Applications (27 Issue 5). https://doi.org/10.1002/met.1955

Hori Y, Cheng VYS, Gough WA, Jien JY, Tsuji LJS (2018) Implications of projected climate change on winter road systems in Ontario's Far North, Canada. Clim Chang https://doi.org/10.1007/s10584-018-2178-2

International Traffic Safety Data and Analysis Group (2020a) *Road safety annual report 2020a*. https://www.itf-oecd.org/sites/default/files/docs/irtad-road-safety-annual-report-2020a_0.pdf

International Traffic Safety Data and Analysis Group (2020b) *Road safety report 2020a | FINLAND*. https://www.itf-oecd.org/sites/default/files/finland-road-safety.pdf

International Traffic Safety Data and Analysis Group (2020c) *Road safety report 2020b | NORWAY*. https://www.itf-oecd.org/sites/default/files/norway-road-safety.pdf

International Traffic Safety Data and Analysis Group (2020d) *Road safety report 2020c | SWEDEN*. https://www.itf-oecd.org/sites/default/files/sweden-road-safety.pdf

Jacobs W, Raatz W (2007) Forecasting road-surface temperatures for different site characteristics. Meteorol Appl 3:243–256. https://doi.org/10.1002/met.5060030306

Juga I, Nurmi P, Hippi M (2013) Statistical modelling of wintertime road surface friction. Meteorol Appl 20:318–329. https://doi.org/10.1002/met.1285

Kangas M, Heikinheimo M, Hippi M (2015) RoadSurf: a modelling system for predicting road weather and road surface conditions. In Meteorological Applications (22 3 544–553). https://doi.org/10.1002/met.1486

Keskinen A (1980) *Costs and benefits of weather service for road winter maintenance in Finland*. https://books.google.com/books/about/Costs_and_Benefits_of_Weather_Service_fo.html?hl=&id=mVnJoQEACAAJLB-cges

Koetse MJ, Rietveld P (2009) The impact of climate change and weather on transport: an overview of empirical findings. Transp Res Part d: Transp Environ 14(3):205–221. https://doi.org/10.1016/j.trd.2008.12.004

Lind P, Belušić D, Christensen O, Dobler A, Kjellström E et al (2020). Benefits and added value of convection-permitting climate modeling over Fenno-Scandinavia. Clim Dyn 55https://doi.org/10.1007/s00382-020-05359-3

Lind P, Lindstedt D, Kjellström E, Jones C (2016) Spatial and temporal characteristics of summer precipitation over Central Europe in a suite of high-resolution climate models. J Clim 29:160308090852005. https://doi.org/10.1175/JCLI-D-15-0463.1

Lind P, Pedersen RA, Kjellström E, Landgren O, Matte D et al (2022) High-resolution convection-permitting climate simulations of the 21st century over Fenno-Scandinavia. Manuscript In Preparation

Lindstedt D, Lind P, Jones C, Kjellström E (2015) A new regional climate model operating at the meso-gamma scale: performance over Europe. Tellus 67https://doi.org/10.3402/tellusa.v67.24138

Matthews L, Andrey J, Picketts I (2017) Planning for winter road maintenance in the context of climate change. Weather, Climate, and Society 9(3):521–532. https://doi.org/10.1175/WCAS-D-16-0103.1

McSweeney RT, Tomlinson JE, Darch GJC, Parker J, Holland T (2016) Impacts of climate change on marginal nights for road salting. Proc Inst Civ Eng Transp 169(2):65–75. https://doi.org/10.1680/jtran.14.00037

Médus E, Thomassen ED, Belušić D, Lind P, Berg P et al (2022) Characteristics of precipitation extremes over the Nordic region: added value of convection-permitting modeling. Nat Hazard 22(3):693–711. https://doi.org/10.5194/NHESS-22-693-2022

Norrman J, Eriksson M, Lindqvist S (2000) Relationships between road slipperiness, traffic accident risk and winter road maintenance activity. In Clim Res (15 185–193). https://doi.org/10.3354/cr015185

Nurmi P, Perrels A, Nurmi V (2013) Expected impacts and value of improvements in weather forecasting on the road transport sector. Meteorol Appl. https://doi.org/10.1002/met.1399

Port and Ocean Engineering under Arctic Conditions (POAC) (2009) The risk of slipping and falling as pedestrian during wintertime. In G. Berggård (Ed.), *Proceedings of the International Conference on Port and Ocean Engineering Under Arctic Conditions* (pp. 126–135). airbanks Institute of Marine Science, University of Alaska. http://worldcat.org/issn/03766756

Ritchie J, Dowlatabadi H (2017) The 1000 GtC coal question: are cases of vastly expanded future coal combustion still plausible? In Energy Economics (65 16–31). https://doi.org/10.1016/j.eneco.2017.04.015

Schwalm CR, Glendon S, Duffy PB (2020) RCP85 tracks cumulative CO emissions. Proc Natl Acad Sci USA 117(33):19656–19657. https://doi.org/10.1073/pnas.2007117117

Screen JA (2014) Arctic amplification decreases temperature variance in northern mid- to high-latitudes. In Nat Clim Chang (4 7 577–582). https://doi.org/10.1038/nclimate2268

Seity Y, Brousseau P, Malardel S, Hello G, Bénard P et al (2011) The AROME-France convective-scale operational model. Mon Weather Rev 139:976–991. https://doi.org/10.1175/2010MWR3425.1

Statistics Finland (2021) Statistics on road traffic accidents. https://findikaattori.fi/en/table/7

Statistics Sweden (2019) Road traffic injuries report 2019. https://www.trafa.se/globalassets/statistik/vagtrafik/vagtrafikskador/2019/vagtrafikskador-2019.pdf

Stocker T, Qin D, Plattner G-K, Tignor M, Allen S et al (2013) IPCC fifth assessment report (AR5) - the physical science basis: annex II - climate system scenario tables: Table AII75. In IPCC AR5. https://doi.org/10.1017/CBO9781107415324.004

Taylor KE, Stouffer RJ, Meehl GA (2012) An overview of CMIP5 and the experiment design. Bull Am Meteor Soc 93(4):485–498. https://doi.org/10.1175/BAMS-D-11-00094.1

Termonia P, Fischer C, Bazile E, Bouyssel F, Brozkova R et al (2018) The ALADIN system and its canonical model configurations AROME CY41T1 and ALARO CY40T1. Geoscientific Model Dev 11:257–281. https://doi.org/10.5194/gmd-11-257-2018

Toivonen E, Hippi M, Korhonen H, Laaksonen A, Kangas M et al (2019) The road weather model RoadSurf (v6.60b) driven by the regional climate model HCLIM38: evaluation over Finland. In Geoscientific Model Development (12 Issue 3481–3501). https://doi.org/10.5194/gmd-12-3481-2019

Yang CH, Yun D-G, Sung J (2012) Validation of a road surface temperature prediction model using real-time weather forecasts. KSCE J Civ Eng 16https://doi.org/10.1007/s12205-012-1649-7